Zoology of instanton solutions in flat potential barriers

Lorenzo Battarra,[1,*] George Lavrelashvili,[2,†] and Jean-Luc Lehners [1,‡]
[1] *Max-Planck-Institut für Gravitationsphysik, Albert-Einstein-Institut Am Mühlenberg 1, D-14476 Potsdam, Germany*
[2] *Department of Theoretical Physics, A.Razmadze Mathematical Institute I.Javakhishvili Tbilisi State University, GE-0177 Tbilisi, Georgia*
(Dated: July 31, 2013)

We perform a detailed study of the existence and the properties of $O(4)$–invariant instanton solutions in Einstein-scalar theory in the presence of flat potential barriers, i.e. barriers where the second derivative of the potential is small at the top of the barrier. We find a whole zoo of solutions: Hawking-Moss, Coleman–De Luccia (CdL), oscillating instantons, asymmetric CdL as well as other non-standard CdL-like solutions with additional negative modes in their spectrum of fluctuations. Our work shows how these different branches of solutions are connected to each other via "critical" instantons possessing an extra zero mode fluctuation. Overall, the space of finite action euclidean solutions to these theories with flat barriers is surprisingly rich and intricate.

I. INTRODUCTION

The problem of tunneling transitions in Einstein–matter theories was first considered in 1980 by Coleman and De Luccia (CdL) in their pioneering article [1]. Their analysis revealed that, as in flat space–time [2], the action of so–called *instanton* solutions - $O(4)$–symmetric euclidean solutions respecting appropriate boundary conditions - determines the tunneling rate and, via analytic continuation, the lorentzian evolution of the bubbles of true vacuum produced by tunneling events. After the CdL instanton another milestone in the investigation of tunneling transitions with gravity was the discovery of the Hawking-Moss (HM) solution [3] which, despite its formal simplicity, raises many questions of interpretation [4].

In recent years the study of tunneling in the presence of gravity has gained new momentum. This renewed attention was triggered on the one side by the string theoretic prediction of a huge landscape of vacua [5, 6] and, on the other side, by the discovery of new types of "oscillating" bounce solutions [7]. A thermal derivation of the CdL tunneling prescription was given in [8], while in [9] different situations in which instanton solutions can disappear under small changes in the potential were considered. A large body of work exists by now discussing cosmological applications of instanton solutions, in particular in the context of false-vacuum eternal inflation – see e.g. [10–14].

In the present paper, we study instanton solutions in general relativity minimally coupled to a scalar field with a very flat potential barrier. By this we mean that we consider potentials that have a vanishing or small second derivative at their maximum value; more explicitly we principally consider potentials of the form

$$V(\varphi) = V_{top} - \frac{\mu^2}{2}\varphi^2 - \frac{1}{p}\varphi^p, \tag{1}$$

with μ^2 small and the two cases $p = 4$, $p = 6$. Compact instantons connecting vacua separated by such relatively flat potential barriers present special properties which were already partially investigated in [7, 15]. We continue this line of research and give a detailed and systematic investigation of these solutions. In doing so, we recover all of the solutions that were previously known: Hawking-Moss, Coleman–De Luccia, oscillating instantons and asymmetric CdL solutions. The entire space of solutions is in fact very complex – for a preview take a look at Figure 10.

We study both the euclidean action and the number of negative fluctuation modes of these solutions in order to determine which solution dominates the tunnelling rate, and which solutions contribute to tunnelling at all. What we find is that these different branches of solutions are connected to one another via "critical " instantons. Such critical instantons contain an extra zero mode fluctuation: one can think of this zero mode as the cross-over moment of the negative fluctuation mode of one branch of solutions evolving into a positive mode of a different branch. In this way, critical instantons connect branches with numbers of $O(4)$–symmetric negative modes that differ by one. The presence of an additional negative mode implies that the euclidean action of that branch of solutions is higher, as the extra negative mode points to the existence of a direction in configuration space along which the action can be lowered.

*Electronic address: lorenzo.battarra@aei.mpg.de
†Electronic address: lavrela@itp.unibe.ch
‡Electronic address: jean-luc.lehners@aei.mpg.de

Thus, instantons with only one negative mode have the lowest action (but if several instantons with equal numbers of negative modes coexist, no argument seems to be known which determines which of these has lowest action).

For oscillating instanton solutions (where the scalar field interpolates more than once between the two sides of the potential barrier), we showed in our previous work that with each additional oscillation a negative mode gets added [16]. Here we also uncover non-standard solutions that look like ordinary CdL solutions in that they are compact and interpolate only once across the potential barrier. Nevertheless, these unusual CdL solutions admit more than one negative fluctuation mode. This highlights the importance of studying the linear fluctuation modes around instanton solutions in order to assess their physical relevance.

The rest of the paper is organized as follows: In Section II we review the basic properties of regular and singular $O(4)$–invariant solutions in Einstein–scalar field theories, as well as the basic undershooting–overshooting arguments. In Section III we present our numerical method and apply it to the case of compact CdL instantons. In Section IV we present numerical results for a flat quartic potential $V = V_{top} - \varphi^4$. In Sections V and VI we generalize our results to the case of nearly flat, asymmetric and positive potentials. Finally, in Section VII we describe the space of instanton solutions in the highly flat potential $V = V_{top} - \varphi^6$. Section VIII contains concluding remarks.

II. INSTANTONS IN EINSTEIN–SCALAR FIELD THEORIES

A. Compact and non–compact solutions

Let us consider the theory of a self–interacting scalar field minimally coupled to gravity defined by the following Euclidean action

$$S_E = \int d^4x\sqrt{g}\left(-\frac{1}{2\kappa}R + \frac{1}{2}\nabla_\mu\varphi\nabla^\mu\varphi + V(\varphi)\right), \tag{2}$$

where $\kappa = 8\pi G_N$ is the reduced Newton's gravitational constant and the potential $V(\varphi)$ will be specified below. The general $O(4)$–invariant euclidean Ansatz

$$\varphi = \varphi(\eta)\,, \tag{3}$$
$$ds^2 = d\eta^2 + \rho^2(\eta)d\Omega_3^2\,, \tag{4}$$

where $d\Omega_3^2$ is the metric on the unit 3–sphere, is a solution of the theory (2) when the field equations are satisfied:

$$\varphi'' = -3\frac{\rho'}{\rho}\varphi' + V_{,\varphi}\,, \tag{5}$$
$$\rho'^2 = 1 + \frac{\kappa\rho^2}{3}\left(\frac{1}{2}\varphi'^2 - V\right). \tag{6}$$

Note that Eq. (5) has a simple mechanical analogy: it describes the motion of a "particle" $\varphi(\eta)$ in an inverted potential $-V(\varphi)$ under a frictional force $3\frac{\rho'}{\rho}$.

It is easy to show that any solution of (5, 6) extends to at least one point where $\rho = 0$: defining $N \equiv \log\rho$ the field equations read

$$\varphi'' = -3N'\varphi' + V_{,\varphi}\,, \tag{7}$$
$$N'^2 - e^{-2N} = \frac{\kappa}{3}\left(\frac{1}{2}\varphi'^2 - V\right). \tag{8}$$

Taking a derivative of (8) and substituting the scalar field equation one gets

$$N'' = -e^{-2N} - \frac{\kappa\varphi'^2}{2}\,. \tag{9}$$

If we consider (9) as a one–dimensional equation of motion, the particle located at $N(\eta)$ is subject to a potential $v(N) = -e^{-2N}/2$ and a time–dependent force pushing it towards negative N: the "potential" is then steep enough for N to reach $N = -\infty$ i.e. $\rho = 0$ in a finite "time", either in the past or the future. The general solution could fail extending to these points if a singularity showed up at a finite value of ρ but, under the assumption that the potential has no singularity at finite φ, this can be proven not to occur (see Appendix A 1). Redefining the sign and the origin of η one can then assume $\rho(\eta = 0) = 0$, and $\rho > 0$ for η positive. Regularity at $\eta = 0$ implies the boundary conditions

$$\varphi'(0) = 0\,, \tag{10}$$
$$\rho'(0) = 1\,, \tag{11}$$

Depending on the value of $\varphi_0 \equiv \varphi(\eta = 0)$ and on the shape of $V(\varphi)$, a solution satisfying these boundary conditions can be *compact* or *non–compact* [17]:

- **compact solutions**: $\rho(\eta)$ reaches a maximum ρ_m and then returns to $\rho = 0$ at some finite "time" $\bar{\eta} > 0$. The existence of such solutions requires V to be strictly positive *somewhere* in field space. Indeed, in this case ρ must have a local maximum at some intermediate value of η and (6) requires $V > 0$ there.

- **non–compact solutions**: $\rho \to \infty$ monotonically as $\eta \to \infty$. The existence of non–compact solutions requires the potential to be negative or zero somewhere. Indeed, in this case $N' > 0$ everywhere and the quantity on the rhs of (8) is monotonically decreasing from its initial value $-\kappa V(\varphi_0)/3$ because of the friction term in (7). If the solution is non–compact the lhs of (8) cannot approach a negative constant, so $V(\varphi_0) \leq 0$. In fact, $V(\varphi_0) = 0$ is compatible with a non–compact solution only when $\varphi(\eta) = \varphi_0$ solves the scalar field equation i.e. when φ_0 is a stationary point of V, in which case the corresponding instanton is four–dimensional flat euclidean space.

Among the one–parameter family of solutions of the field equations obeying (10), (11), the ones which may be relevant for tunneling are those which respect the same boundary conditions as the false vacuum euclidean geometry, whose action enters in the expression of the decay rate

$$\Gamma \propto \exp\left\{-\left(S_E(\varphi) - S_E(\varphi_{fv})\right)\right\}\,. \tag{12}$$

These special solutions of the field equations are referred to as *instantons*. Compact solutions, which describe tunneling from de Sitter space and will be the focus of this paper, have the topology of a four–sphere whose "north pole" can be taken to be $\eta = 0$. In this case, the natural boundary condition is the requirement of regularity at the "south pole" $\rho(\bar{\eta}) = 0$ of the euclidean geometry:

$$\rho'(\bar{\eta}) = -1\,, \tag{13}$$
$$\varphi'(\bar{\eta}) = 0\,. \tag{14}$$

When the scalar potential is everywhere well–defined, these conditions can be shown to be equivalent to requiring a finite limit $\bar{\varphi}_0 \equiv \lim_{\eta\to\bar{\eta}} \varphi(\eta)$ for the scalar field (see Appendix A 2). Unlike for the non–compact case, for compact instantons the scalar field cannot approach a stationary point of V at the south pole $\eta = \bar{\eta}$. Thus $\bar{\varphi}_0 \equiv \varphi(\bar{\eta})$ is always different from the false vacuum value and, as described in [8], a thermal fluctuation from the minimum of the potential to $\bar{\varphi}_0$ is needed to initiate tunneling from de Sitter space. Moreover, the similarity of the boundary conditions (13, 14) and (10, 11) and the invariance of the field equations under $\eta \to \bar{\eta} - \eta$ imply that if φ_0 corresponds to a regular solution so does $\bar{\varphi}_0$.

B. Overshooting and undershooting

The existence of instanton solutions is usually proven through the so–called *overshooting–undershooting* argument [1]. For each value of $\varphi_0 \equiv \varphi(\eta = 0)$, a unique solution of the field equations can be found with initial conditions (10), (11). For generic values of φ_0, however, the solution will not respect the boundary conditions at $\eta = \bar{\eta}$. In the compact case, this means that generically $\varphi \to \pm\infty$ as $\eta \to \bar{\eta}$. Across a discrete set of values $\{\varphi_0^i\}$ however, the sign of this divergence changes, e.g.:

$$\varphi \overset{\eta\to\bar{\eta}}{\longrightarrow} +\infty, \qquad \varphi_0 < \varphi_0^i\,, \tag{15}$$
$$\varphi \overset{\eta\to\bar{\eta}}{\longrightarrow} -\infty, \qquad \varphi_0 > \varphi_0^i\,. \tag{16}$$

From the continuous dependence of the solution on the parameter φ_0 one deduces that the solution corresponding to each separating value φ_0^i cannot have either divergent behavior, hence it is necessarily regular. A transition from (15) to (16) is always associated with a change in the *number of oscillations* or *number of passes* n of the scalar field, conventionally defined as the number of zeros of φ' plus one (excepting the boundary condition zero $\varphi'(0) = 0$ and the possible one at $\eta = \bar{\eta}$), in such a way that an instanton with a monotonically varying scalar field has $n = 1$. In the compact case, instantons appear at those special values of φ_0 across which the discrete function $n(\varphi_0)$ has a jump. In particular, based on the analysis of perturbations of the regular solutions, one can show that n can only jump by a unit value [17]: a transition like (15) (16) is necessary and sufficient for the existence of an instanton solution, whose

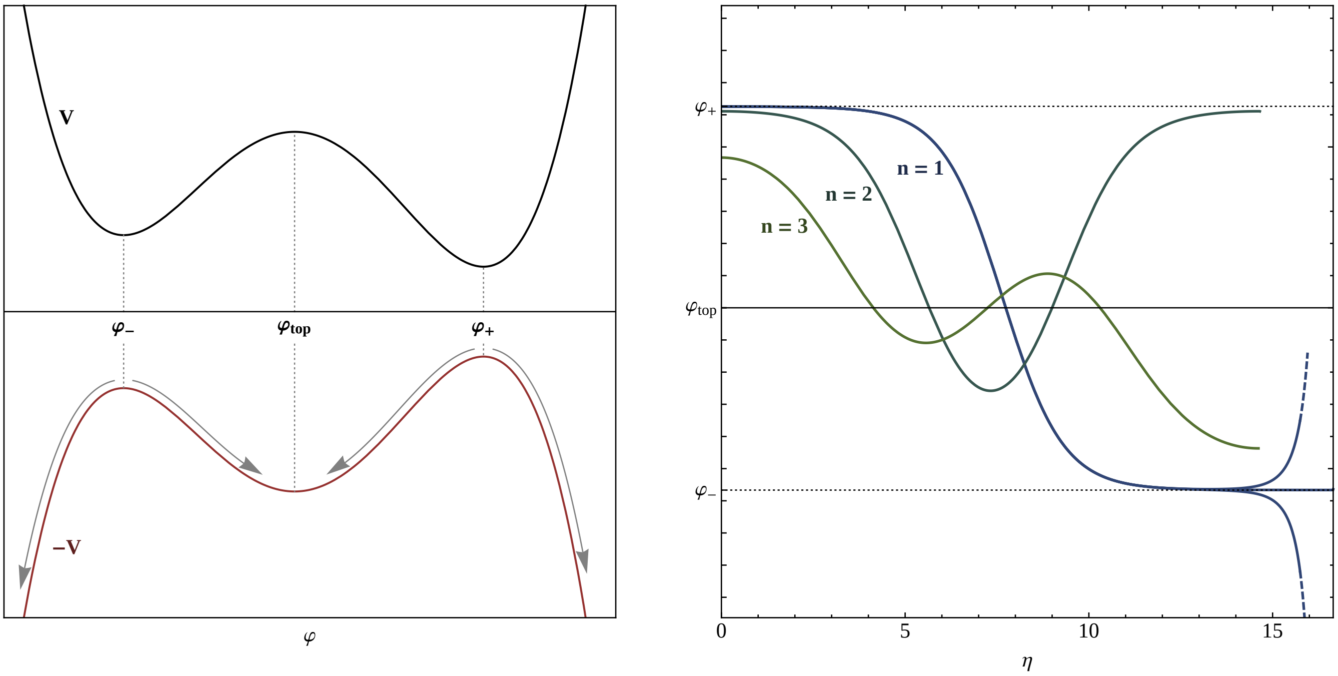

Figure 1: Left panel: double well–potential and its euclidean version (red). Right panel: profiles of three instanton solutions for the potential (20), with $\xi = 0.1$, $V_{top} = e^{-2}$ and $V_{top}/V_+ = 4$. The appearance of the $n = 1$ as separating solution between $n = 1$ and $n = 2$ is highlighted (see also Figure 2).

number of oscillations is $\min\{n(\varphi_0^i - \epsilon), n(\varphi_0^i + \epsilon)\}$ [1].

Overshooting–undershooting arguments prove the existence of jumps in $n(\varphi_0)$, hence the existence of an instanton solution, by showing that $n(\varphi_0)$ takes different values at special points in field space. The simplest example of such an argument applies to vacuum decay in flat–space [2]. Consider a simple double–well potential as in Figure 1. The equation for the scalar field reads

$$\varphi'' + \frac{3}{\eta}\varphi' = V'(\varphi) \ . \tag{17}$$

This is the equation for a particle subject to a potential $-V$ and a friction force with coefficient $3/\eta$. If φ_0 is set close enough to φ_{top}, the scalar field will not escape from the euclidean potential well and will undergo an infinite number of damped oscillations, hence $n(\varphi_{top} + \epsilon) = \infty$ (*undershooting*). On the other hand, if φ_0 is set very close to the local maximum φ_+ of the inverted potential, the scalar field will escape from it at arbitrarily large η:

$$\eta_{escape} \gtrsim -\frac{1}{|V''(\varphi_{top})|^{1/2}} \log\left(\varphi_+ - \varphi_0\right) \ . \tag{18}$$

In this way, the friction coefficient can be made arbitrarily small during the non–trivial part of the scalar field evolution, and provided [2] $V_+ < V_-$ the scalar field can go beyond φ_- and then diverge as the potential increases again (*overshooting*). Therefore, $n(\varphi_0 = \varphi_+ - \epsilon) = 1$ and an $n = 1$ instanton must separate the undershooting and overshooting regimes.

---

[1] The non–compact case can be very different. For example, $n(\varphi_0)$ can jump by more than unity [17]. Moreover, depending on the shape of the potential and on the boundary conditions at $\eta = \bar{\eta} = \infty$, the existence of instanton solutions may not require any jump in $n(\varphi_0)$.

[2] Our notation should be obvious: $V(\varphi_\pm) \equiv V_\pm, V(\varphi_{top}) \equiv V_{top}$, and $V(\varphi_0) \equiv V_0$.

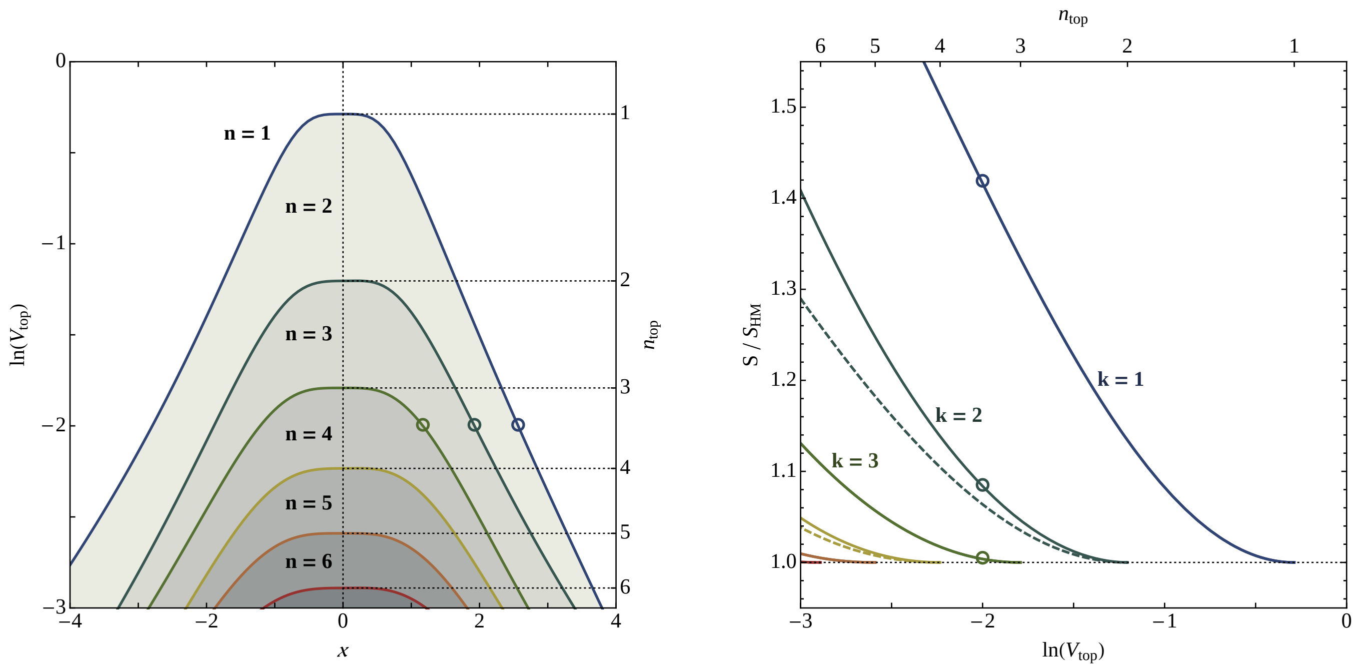

Figure 2: Left panel: level lines of $n(x, V_{top})$ for the potential (20) with $\xi = 0.1$ and $V_{top}/V_+ = 4$. The three circles correspond to the solutions represented in the right panel of Figure 1. Right panel: euclidean action of the different branches of instanton solutions normalized to the action of the corresponding Hawking–Moss instanton. Solid lines (resp. dashed lines) represent the instantons with $x > 0$ (resp. $x < 0$). The number of negative modes k is also indicated.

III. STANDARD COMPACT CDL SOLUTIONS

A. Overshooting and undershooting in de Sitter space

When gravity is taken into account and the potential allows only compact instantons, as the one in Figure 1, both ends of the undershooting–overshooting argument need to be updated. All solutions being compact, the friction coefficient ρ'/ρ becomes negative before $\eta = \bar{\eta}$ (*anti–friction*) and the scalar field diverges except when the solution is regular. Therefore, for φ_0 very close to φ_{top} the number of oscillations $n(\varphi_0)$ remains finite. Its value depends on the shape and value of the potential at the top of the barrier $\varphi = \varphi_{top}$, and was determined [7] to be the smallest integer n_{top} satisfying

$$n_{top}(n_{top} + 3) > \frac{|V''_{top}|}{H^2_{top}}, \quad H_{top} \equiv \sqrt{\frac{\kappa V_{top}}{3}} \,. \tag{19}$$

This relation translates the fact that only a finite number of oscillations around φ_{top} can be fit in the Hubble radius H^{-1}_{top} of the compact geometry, before anti–friction kicks the scalar field away from the top of the potential barrier. At the other end of field space, namely for $\varphi = \varphi_+ - \epsilon$, the overshooting argument applies in a stronger form than in flat space: even if $V_+ \geq V_-$, one finds $n(\varphi_0 \lesssim \varphi_+) = 1$ provided $V_+ > 0$. Indeed, if the scalar field is initially set very close to φ_+, the naively expected escape time (18) can exceed the Hubble radius H_+^{-1}. In this case the scalar field is kicked away from φ_+ by the divergent anti–friction force: by decreasing $(\varphi_+ - \varphi_0)$ this kick can be made large enough to let the scalar field go over φ_- and diverge monotonically. This means that $n(\varphi_0)$ varies between n_{top} and 1 as φ_0 varies between φ_{top} and φ_+. Hence, an odd number of instantons with $\varphi_{top} < \varphi_0 < \varphi_+$ exists for each value of n between 1 and $n_{top} - 1$ (including both extrema). The same conclusion clearly applies to the part of the potential between φ_- and φ_{top}.

B. Instanton diagrams

In many cases, *exactly* one instanton exists for every n between 1 and $n_{top} - 1$. As an example, consider the potential

$$V = V_{top} - \frac{1}{2}\varphi^2 - \frac{\lambda^{1/2}\xi}{3}\varphi^3 + \frac{\lambda}{4}\varphi^4 \,. \tag{20}$$

The left panel of Figure 2 depicts an *instanton diagram*, representing contour lines of n as a function of V_{top} and the x variable defined by:

$$\varphi_0 = \begin{cases} \varphi_+ \left(1 - e^{-x^2}\right), & x > 0 \,, \\ \varphi_- \left(1 - e^{-x^2}\right), & x < 0 \,. \end{cases} \tag{21}$$

The use of this logarithmic variable is particularly helpful because instanton initial values φ_0 tend to accumulate near the vacuum values $\varphi_\pm$. The parameter λ is adjusted to keep the ratio $r = V_+/V_{top}$ constant and equal to $1/4$, and we set $\xi = 0.1$, $\kappa = 1$. In order to obtain the instanton diagram numerically, the function $n(x, V_{top})$ is sampled on a grid of values of (x, V_{top}): at each point of the grid, n is obtained by solving the field equations and counting the number of oscillations. A more accurate estimate for the values of φ_0 corresponding to particular instantons can then be obtained by using bisection algorithms with the diagram as guide. This method for visualizing the location of instanton solutions in field/parameter space was first proposed in [17]. For potentials admitting a simple range of instanton solutions the method only brings a different way to visualize their location in field/parameter space. On the other hand, in the case of flat potential barriers this visualization is extremely helpful in understanding the nature of various non–standard solutions, which are the subject of the next sections.

C. Zero and negative modes

As V_{top} decreases, n_{top} (which we defined in (19)) increases and more and more instanton solutions appear, moving away from the Hawking–Moss (HM) solutions $\varphi = \varphi_{top}$ located at:

$$V_n = \frac{|V''_{top}|}{\kappa} \frac{3}{n(n+3)} \,, \tag{22}$$

$$\rho_n = H_n^{-1} \sin\left(H_n \eta\right), \quad H_n = \sqrt{\frac{\kappa V_n}{3}} \,. \tag{23}$$

These HM solutions are called *critical* because they possess an $O(4)$–invariant perturbation zero mode of the scalar field, which corresponds to an infinitesimal displacement along the instanton curve passing through the $x = 0$ axis. Even away from these special HM points, the presence of a regular perturbation mode is signaled on the diagram by the horizontal slope of the instanton curve (see Appendix B), and the corresponding instanton is called *critical*. Indeed, in this case the infinitesimal displacement along the instanton curve leaves the parameters of the theory unchanged and modifies the regular solution into an infinitesimally different one, still respecting regularity and $O(4)$ invariance.

It follows from this observation that all the instantons located on a single curve in the diagram of Figure 2 possess the same number of *negative modes* in the $O(4)$–invariant sector of the scalar field perturbations. Denoting the gauge-invariant scalar fluctuation mode by f, it satisfies the equation [18–22]

$$- f'' + U[\rho(\eta), \varphi(\eta)] f = \epsilon\, f \,, \tag{24}$$

with eigenvalue ϵ and effective potential

$$\begin{aligned} U[\rho(\eta), \varphi(\eta)] \;&\equiv\; \frac{1}{\mathcal{Q}} V_{,\varphi\varphi} - \frac{10\rho'^2}{\rho^2 \mathcal{Q}} + \frac{12\rho'^2}{\rho^2 \mathcal{Q}^2} + \frac{8}{\rho^2 \mathcal{Q}} - \frac{6}{\rho^2} - \frac{3\mathcal{Q}}{\rho^2} - \frac{\rho'^2}{4\rho^2} \\ &\quad + \frac{\kappa \rho^2}{2\mathcal{Q}^2} V_{,\varphi}^2 - \frac{2\kappa \rho \rho' \varphi'}{\mathcal{Q}^2} V_{,\varphi} - \frac{\kappa}{6}\left(\varphi'^2 + V\right) \,, \end{aligned} \tag{25}$$

$$\mathcal{Q} \;\equiv\; 1 - \frac{\kappa \rho^2 \varphi'^2}{6} \,. \tag{26}$$

A property of this equation is that the eigenvalues $\{\epsilon^i\}_{i=1,2,\ldots}$ of different families of solutions vary continuously on each family. Therefore, additional negative eigenvalues can only appear at critical points corresponding to instantons possessing a *zero mode*, i.e. a regular perturbation mode.

In the case described in Figure 2, the number k of $O(4)$–invariant negative modes turns out to be equal to the number of oscillations of the respective instantons (see [16] for a detailed study of these negative modes), i.e. $k = n$. Moreover, as shown in the right panel of Figure 2, the euclidean action of the $n = 1$ solutions turns out to be always

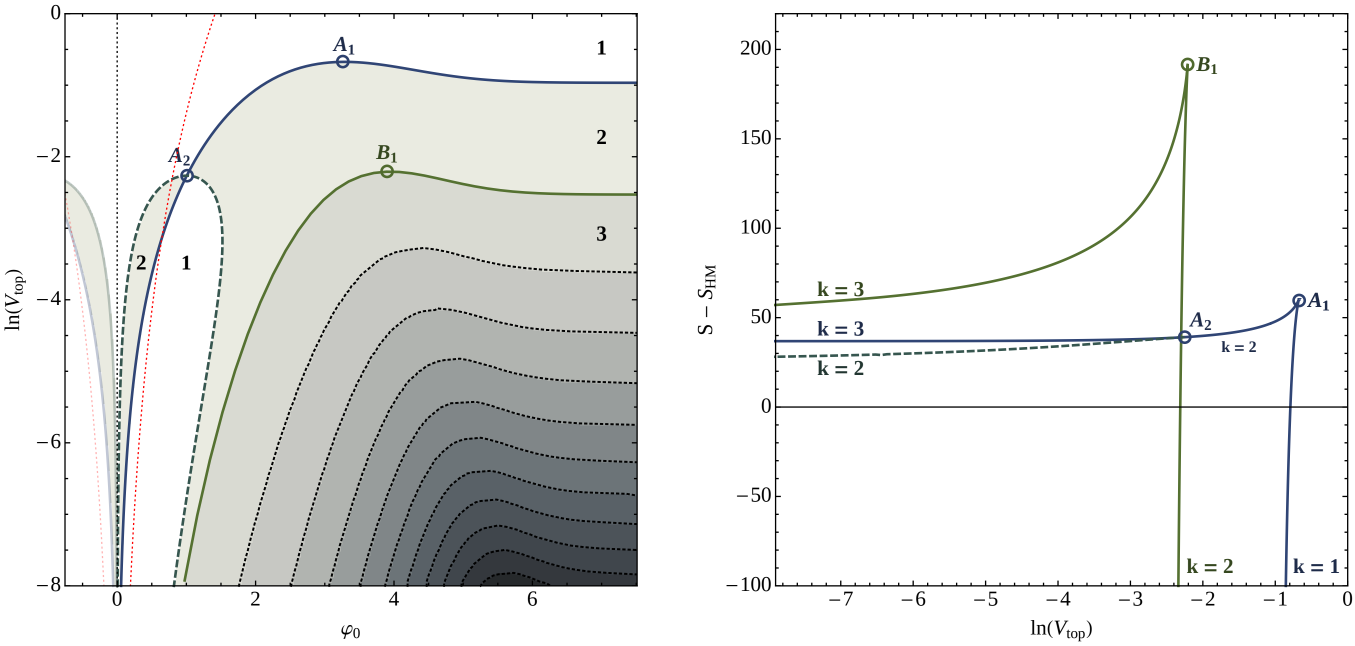

Figure 3: Left panel: instanton diagram for the potential (30), with the choice of units $\lambda = \kappa = 1$. The red, dotted line represents $V = 0$. The asymmetric solutions mentioned in the text correspond to the dashed line emanating from the bifurcation point A_2; these solutions interpolate between two values $\pm\varphi_1, \mp\varphi_2$, where φ_1, φ_2 are the intersections of a horizontal line and the dashed line. Right panel: difference between euclidean action of the $n = 1$ and $n = 2$ solutions and the corresponding HM solutions; the number of negative modes, k, is also indicated.

the most negative and, in particular, to be more negative than the action of the corresponding HM solutions,

$$S_{HM} = -\frac{24\pi^2}{\kappa^2 V_{top}} \,. \tag{27}$$

Therefore the $n = 1$ instantons are the solutions which determine the tunneling rate in the theory specified by the potential (20), and they are commonly referred to as Coleman–de Luccia instantons.

IV. TUNNELING THROUGH FLAT BARRIERS: QUARTIC POTENTIAL

The case we just described is the simplest one compatible with the values of $n(\varphi_0)$ obtained from the undershooting–overshooting arguments: $n(\varphi_0)$ grows monotonically from $1 = n(\varphi_+ - \epsilon)$ to $n_{top} = n(\varphi_{top} + \epsilon)$. However, sufficient conditions on the shape of the potential are not known which guarantee this behavior of $n(\varphi_0)$. In particular, when $n_{top} = 1$ the number of instantons of any order n with $\varphi_{top} < \varphi_0 < \varphi_+$ is constrained to be an *even* integer, but the undershooting–overshooting argument does not force it to vanish. The corresponding potentials are characterized by a *flat* barrier separating the two vacua:

$$\frac{3|V''_{top}|}{\kappa V_{top}} \leq 4 \,. \tag{28}$$

A particular case of exactly flat potential was studied in [15], where the existence of several $n = 1$ solutions was established despite $n_{top} = 1$. In particular, it was shown that these solutions have more negative euclidean action than the corresponding HM solution. In [7] similar results were found together with other non–standard behaviors of the $n(\varphi_0)$ function. Moreover, the authors suggested the existence of a generalized bound on the curvature of the potential *around* the top of the barrier for the existence of $n = 1$ instantons. However, the only analytic result known so far is a *necessary* condition, stating that the inequality

$$\frac{3|V''(\varphi)|}{\kappa V(\varphi)} > 4 \,, \tag{29}$$

must be satisfied for some value of φ in order for $n = 1$ solutions to exist [23].

In order to reconsider the question of tunneling through flat barriers, we start from the simple quartic potential

$$V = V_{top} - \frac{\lambda}{4}\varphi^4, \quad \lambda > 0\,. \tag{30}$$

In flat space ($\kappa = 0$), the conformal invariance of the scalar field theory allows for the existence of a continuous family of instanton solutions [24], called *Fubini* instantons, for which the scalar field approaches $\varphi_{top} = 0$ asymptotically:

$$\varphi_b(\eta) = \sqrt{\frac{8}{\lambda}}\frac{b}{\eta^2 + b^2}, \quad b \in \mathbb{R}\,. \tag{31}$$

In fact S. Fubini found these finite action euclidean solutions in scalar field theory with conformally invariant (quartic) potential almost at the same time as instantons were discovered in the Yang-Mills theory [25]. Later Fubini instantons were rediscovered several times [26, 27]. They describe tunneling without barrier [27–29], and have applications in particle physics as well as in the context of the AdS/CFT conjecture [30–33]. Moreover, it was suggested [34] that Fubini vacua can be used as classical de Sitter vacua.

It is easy to prove that Fubini instantons have one negative mode in their spectrum of linear perturbations (such solutions are also commonly referred to as *bounces*). Indeed, all Fubini instantons possess a regular zero mode f_b corresponding to an infinitesimal displacement along the family of solutions,

$$f_b = \partial_b \varphi_b = \sqrt{\frac{8}{\lambda}}\frac{\eta^2 - b^2}{(\eta^2 + b^2)^2}\,. \tag{32}$$

Each such zero mode has a single node at $\eta = b$ and hence, according to nodal theorems, there must exist one node-free solution with a lower eigenvalue – in other words, each Fubini instanton possesses a single negative mode.

When gravity is included, this picture changes radically: conformal invariance is lost and at most a finite number of instantons is left [35]. Via the rescalings

$$g_{\mu\nu} \equiv \frac{\kappa}{\lambda}\tilde{g}_{\mu\nu}\,, \quad \varphi \;\equiv\; \kappa^{-1/2}\tilde{\varphi}\,, \tag{33}$$

one can set $\lambda = \kappa = 1$. The rescaling produces a multiplicative factor in front of the euclidean action

$$S_{\kappa,\lambda,V_{top}}[g_{\mu\nu}, \varphi] = \lambda^{-1} S_{1,1,\bar{V}_{top}}[\tilde{g}_{\mu\nu}, \tilde{\varphi}], \quad \bar{V}_{top} = \frac{\kappa^2 V_{top}}{\lambda}\,, \tag{34}$$

which does not modify any conclusion regarding the existence of instanton solutions, their relative contribution to the tunneling rate or the spectrum of their negative modes. From now on, we will drop bars and denote by V_{top} the reduced parameter appearing in the action when $\lambda = \kappa = 1$.

Assuming $V_{top} > 0$, one can easily show that the general $O(4)$–invariant solution is compact. Indeed, in a non–compact solution the scalar field generally approaches a stationary point of the potential. As the only stationary point for the potential (30) is located at $V > 0$, the corresponding asymptotic geometry cannot be non–compact. The instanton diagram obtained with this potential is plotted in Figure 3. Because of the symmetry of the potential the diagram is also symmetric under $\varphi_0 \to -\varphi_0$. The manifest differences with respect to standard case of Figure 2 can already be partially explained in terms of the expected behavior of $n(\varphi_0)$ at the two extrema of field space:

- $\varphi_0 = \varphi_{top} + \epsilon$: the flatness of the potential near φ_{top} implies $n_{top} = 1$. For this reason, all the instanton curves bend and do not cross the vertical axis. This corresponds to the fact that small perturbations of the scalar field around the HM solution $\varphi = 0$ always "overshoot" without oscillating. Indeed, the time–scale for the potential–induced oscillations to start is roughly

$$\eta_{osc} \sim |V_{,\varphi\varphi}(\varphi_0)|^{-1/2} \sim |\varphi_0|^{-1} \tag{35}$$

  Hence, if φ_0 is made small enough, η_{osc} can be made arbitrarily larger than the HM Hubble radius, and the anti–friction term makes the scalar field diverge before the oscillations start.

- $\varphi_0 \to \varphi_+ = \infty$: in this limit the overshooting argument clearly does not apply, because the asymptotic geometry is generally that of euclidean anti–de Sitter space, hence we generally find $n(\varphi_0) > 1$ for large values of φ_0. Instead, the instanton curves approach horizontal asymptotes. This means that the shift $\varphi_0 \to \varphi_0 + c$ becomes an approximate solution–generating transformation. Indeed, the corresponding solutions consist of two large patches of slow–roll pseudo–inflationary solutions in the potential $-V \sim \varphi^4$, glued together by a "wall" consisting of the scalar field evolution near $\varphi = \varphi_{top}$.

All the solutions represented in Figure 3, except the "strange" $n = 1$ solutions represented by a dashed line, are

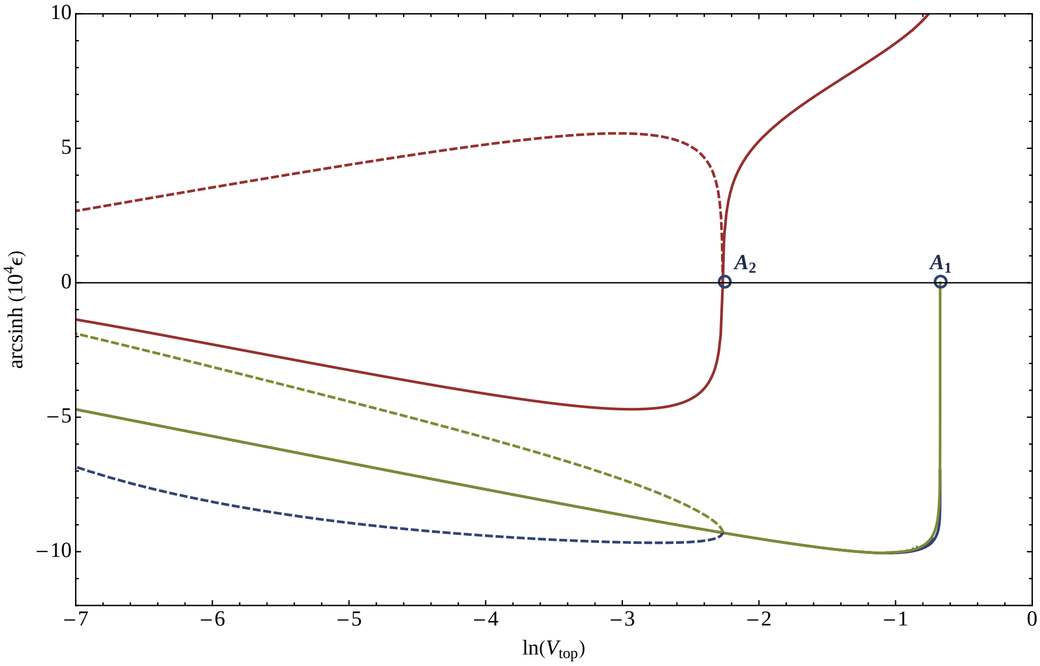

Figure 4: Behavior of the lowest three eigenvalues ϵ of the equation (24) for $O(4)$–invariant perturbations, for the $n = 1$ instantons backgrounds. Dashed lines correspond to the solutions plotted dashed lines in the left panel of Figure 3. The two lowest eigenvalues along the symmetric branch are almost coincident, except near the point A_1 where the second eigenvalue approaches zero.

symmetric under $\varphi \to -\varphi$, $\eta \to \bar{\eta} - \eta$, namely:

$$\eta \;\to\; \bar{\eta} - \eta \,, \tag{36}$$

$$\varphi \;\to\; (-1)^n \varphi \,. \tag{37}$$

In particular, they connect $\varphi_0 \equiv \varphi(\eta = 0)$ to $\bar{\varphi}_0 \equiv \varphi(\bar{\eta}) = (-1)^n \varphi_0$. The "strange" solutions appear from the bifurcation point A_2 and connect the values of φ_0 on one side of that point to minus the values on the opposite side, see Figure 3. The appearance of this bifurcation point and the asymmetry of the corresponding solutions despite the symmetry of the potential (first noticed in [7]) could not be observed for the $n > 1$ branches in the interval of parameters we considered, but may exist at smaller values of V_{top}.

All the non–standard solutions located on the left of the points A_1, $B_1, \ldots$ turn out to have higher euclidean action than the corresponding HM instanton (see the right panel of Figure 3). Moreover, focusing on the $n = 1$ solutions, we observed that across the points A_1 and A_2 additional negative modes appear. In particular, the symmetric branch possesses two negative modes between A_1 and A_2, and three negative modes below A_2. Indeed, in agreement with our expectations, at these two points the horizontal slope of an instanton curve signals the presence of a zero mode: the instantons located at A_1 and A_2 are *critical* solutions. On the other hand, the asymmetric $n = 1$ branch possesses two negative modes, and has lower euclidean action than the symmetric one (see the right panel of Figure 3). For this reason, the additional negative mode of the latter can then be interpreted as the perturbation generating the transition from the symmetric to the non–symmetric branch.

This qualitative analysis is confirmed by an explicit computation, along the different $n = 1$ branches, of the three lowest eigenvalues of the perturbation equation (24) (see Figure 4). Across A_1 and A_2, a positive eigenvalues becomes negative on the symmetric branch.[3] These results show that the number of negative modes can be different from the number of oscillations of an instanton solution. Furthermore, several solutions with the same number of negative modes can co–exist: e.g. the $n = 1$ symmetric solutions below A_2 and the $n = 2$ solutions on the left of B_1, both possessing three negative modes.

The solutions located on the right of the points A_1, $B_1, \ldots$ appear as standard CdL solutions, for which the number of negative modes k coincides with the number of oscillations n. However, as the potential (30) is unbounded from

[3] Note that on the right of A_1, the computation of the negative modes according to (24) becomes inconsistent, as the $\mathcal{Q}$ function appearing in the perturbation potential becomes negative in a finite range of values of η. How to consistently work out the perturbation modes in this case is currently an open problem.

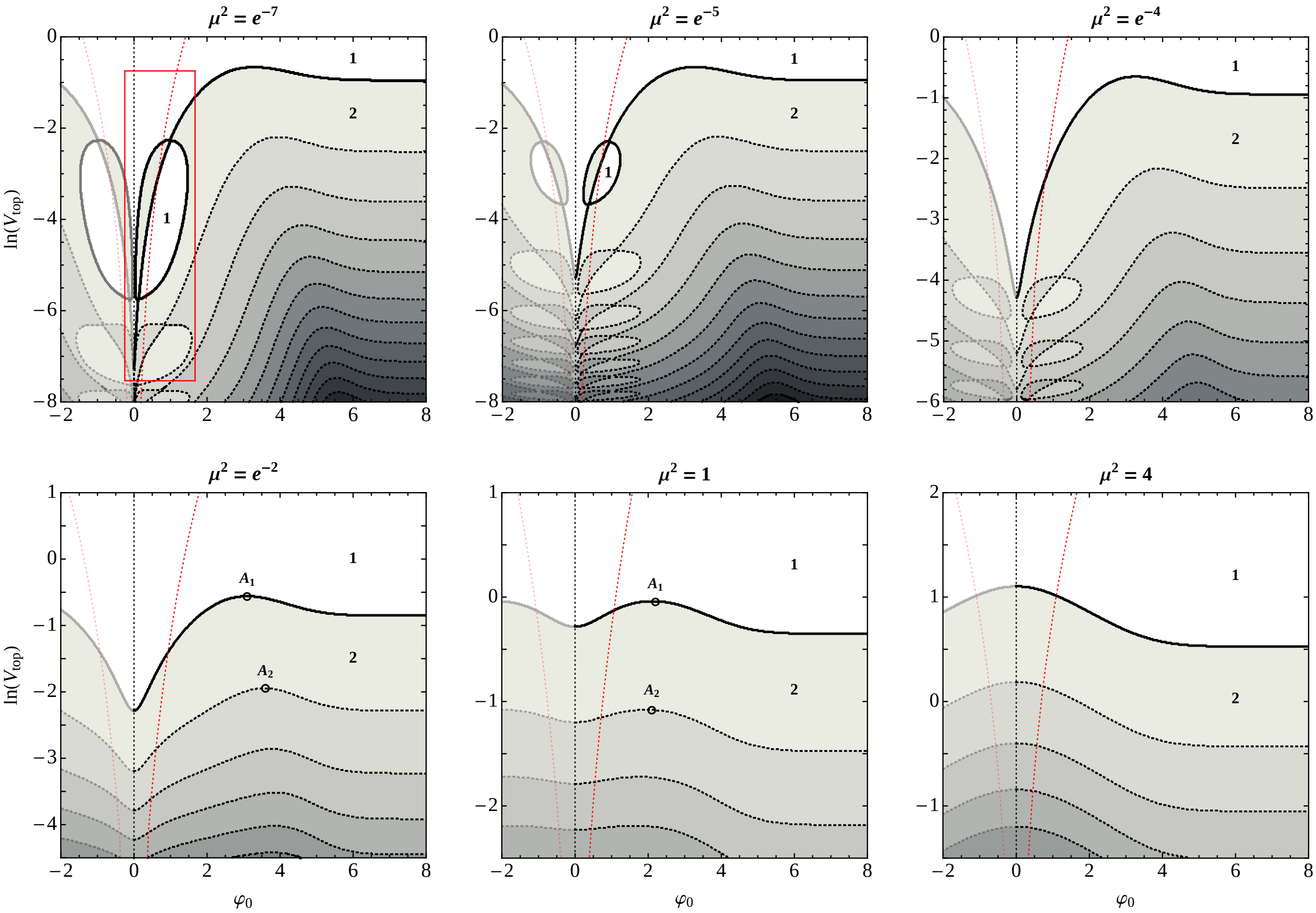

Figure 5: Instanton diagrams for various values of the reduced mass parameter μ^2 in the potential (39). The red, dotted lines represent $V(\varphi_0) = 0$ as in Figure 3. The region enclosed in the red box in the top, leftmost panel is depicted in the left panel of Figure 6.

below, they only exist in small ranges of values of V_{top}. Moreover, as shown in Figure 3, the scalar field takes values for which the potential is negative for all these solutions, which are therefore not directly relevant for tunneling from de Sitter to de Sitter/Minkowski space.

Furthermore, since the potential is exactly flat at the top ($V''(\varphi_{top}) = 0$), the Hawking-Moss instanton does not contain a negative mode. This implies that across the entire region where the potential (30) is positive, no instantons exist which possess a single negative mode in their spectrum. Thus it appears that these regions correspond to "mountains" of semi-classical stability. It will be of interest to explore what role these might play in a landscape/eternal inflation context.

V. INTERMEDIATE CASE: $V = V_{top} - \frac{\mu^2}{2}\varphi^2 - \frac{1}{4}\varphi^4$

In the previous section we have seen that the flatness of the potential at φ_{top} allows the existence of critical instantons with a non–trivial scalar field and, correspondingly, the presence of new instanton branches with additional negative modes. It is then natural to ask how this picture evolves to the standard one when the curvature of the potential is increased from zero.

To address this question, we consider the potential

$$V = V_{top} - \frac{\mu^2}{2}\varphi^2 - \frac{\lambda}{4}\varphi^4 \,. \tag{38}$$

As in the previous case, by an appropriate choice of units we may set $\lambda = \kappa = 1$,

$$V = \bar{V}_{top} - \frac{\bar{\mu}^2}{2}\varphi^2 - \frac{1}{4}\varphi^4 \,. \tag{39}$$

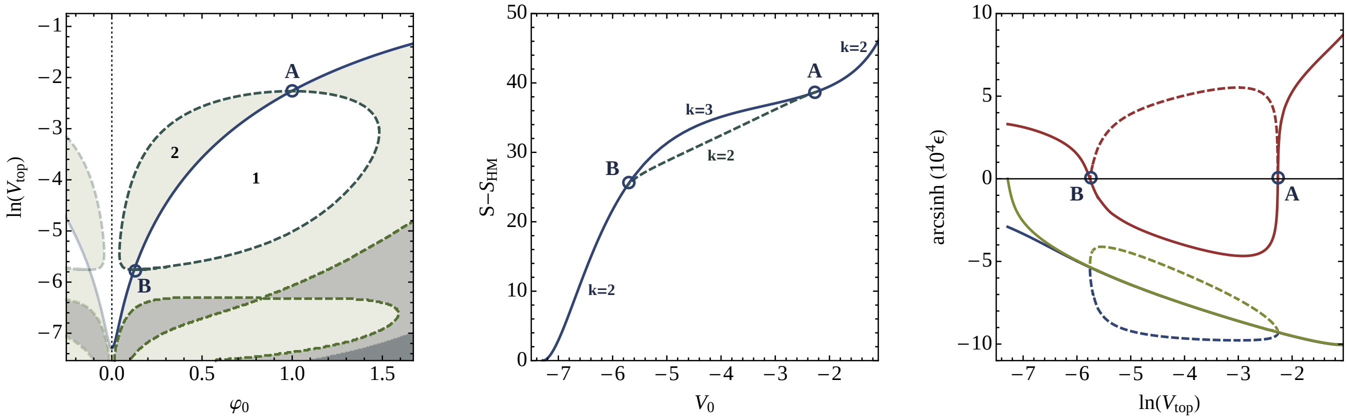

Figure 6: Left panel: detail of the instanton diagram for $\mu^2 = e^{-7}$ (see Figure 5). Center panel: difference between the euclidean action of the $n = 1$ instantons and the corresponding HM solutions across the critical points A and B. Right panel: three lowest eigenvalues of the $n = 1$ instanton solutions; dashed lines correspond to the non–symmetric $n = 1$ solutions depicted in dashed lines on the left panel.

The rescaled parameters appearing in (38) are related to the original parameters by

$$\bar{V}_{top} = \frac{\kappa^2 V_{top}}{\lambda} , \tag{40}$$

$$\bar{\mu}^2 = \frac{\kappa \mu^2}{\lambda} . \tag{41}$$

Using the same argument as for the $\mu^2 = 0$ case, one can easily prove that all $O(4)$–invariant solutions of the field equations with the potential (38) are compact.

In Figure 5 we present several instanton diagrams corresponding to different values of μ^2. The presence of a mass term allows $n(\varphi_{top} + \epsilon)$ to take values greater than one for sufficiently small V_{top}, in agreement with (19). In the instanton diagrams, this is related to the fact that the instanton curves now join the $\varphi = 0$ axis, and thus they are continuously related to the HM critical solutions, like in the standard case depicted in Figure 2.

For small values of μ^2, the bifurcation corresponding to the critical point along the $n = 1$ curve is now associated to a second bifurcation at smaller values of V_{top}, giving rise to a ring–like structure (see also Figure 6). The same structure appears on all the $n > 1$ branches we were able to explore, suggesting that a single bifurcation should also be present, at values of V_{top} below our numerical limitations, in the $\mu^2 = 0$ case. In going through the ring in the direction of decreasing V_{top}, the symmetric branches acquire an additional negative mode and, correspondingly, their euclidean action is greater than that of the corresponding non–symmetric branches (Figure 6, center panel). The eigenvalue associated to this mode turns positive again across the new bifurcation point, close to the critical HM solution (Figure 6, right panel). For these small values of μ^2, the properties of the solutions located at larger φ_0 remain the same as in the $\mu^2 = 0$ case, discussed in the previous section. Moreover, also like in the massless case, the non–standard solutions appearing on the left of the critical points $A_1, A_2, \ldots$ always have greater euclidean action than the corresponding HM instantons.

When μ^2 is increased, the ring–like structures gradually shrink and disappear, starting from the one located on the $n = 1$ branch. Moreover, at the critical values $\mu_{c,1}, \mu_{c,2}, \ldots$, the critical instantons located at $A_1, A_2, \ldots$ approach the $\varphi_0 = 0$ axis and "disappear" by joining the critical HM solutions. For this reason, when $\mu > \mu_{c,n}$ the non–standard branches are no longer present and only "standard" n–oscillating instantons with $k = n$ negative modes survive: $n_{top} > 1$ is again a necessary condition for the existence of solutions. In this regime, except for the different behavior at large φ_0 due to the unboundedness of the potential, the instanton diagrams are qualitatively similar to the one presented in Figure 2.

The critical values μ_n^c can be determined by analyzing the perturbations of the critical HM solutions. Indeed, as one can clearly see in Figure 5, a small perturbation of the n–critical HM instanton will result in a singular $n + 1$ (resp. n) solution if $\mu < \mu_{c,n}$ (resp. $\mu > \mu_{c,n}$). More precisely, the behavior of the curve of n–oscillating instantons at small $(\varphi_0 - \varphi_{top})$ is determined by the number of oscillations of the solutions:

$$\varphi = \varphi(\eta, \varphi_0) , \tag{42}$$

$$\rho = \rho(\eta, \varphi_0) , \tag{43}$$

in the theory admitting the n–critical HM solution

$$n(n+3) = \frac{3\mu^2}{\kappa V_n} \,. \tag{44}$$

For small φ_0, the solution (42,43) can be written as an expansion in the value of $(\varphi_0 - \varphi_{top})$:

$$\begin{aligned} \varphi(\eta,\varphi_0) &= \varphi_{top} + (\varphi_0 - \varphi_{top})\,\varphi_{(1)}(\eta) + (\varphi_0 - \varphi_{top})^2\,\varphi_{(2)}(\eta) + \dots \,, && (45)\\ \rho(\eta,\varphi_0) &= \rho_{HM} + (\varphi_0 - \varphi_{top})\,\rho_{(1)}(\eta) + (\varphi_0 - \varphi_{top})^2\,\rho_{(2)}(\eta) + \dots \,. && (46)\end{aligned}$$

The functional coefficients $(\varphi_{(k)}, \rho_{(k)})_{k\geq 1}$ are the k–th order $O(4)$–invariant perturbations of the background critical HM solution:

$$\rho_{HM} = H_n \sin(H_n \eta), \quad H_n = \left(\frac{\mu^2}{n(n+3)}\right)^{1/2} \,. \tag{47}$$

The boundary conditions specifying these perturbation modes follow from those for the full solution:

$$\begin{aligned} \varphi(\eta = 0, \varphi_0) = \varphi_0 \quad &\Longrightarrow \quad \begin{cases} \varphi_{(1)}(0) = 1\,, \\ \varphi_{(k)}(0) = 0, \quad k > 1\,, \end{cases} && (48)\\ \rho(\eta = 0, \varphi_0) = 0 \quad &\Longrightarrow \quad \rho_{(k)}(0) = 0\,, && (49)\\ \rho'(\eta = 0, \varphi_0) = 1 \quad &\Longrightarrow \quad \rho'_{(k)}(0) = 0\,. && (50)\end{aligned}$$

For general values of φ_0, we expect the solution (42) to be singular. This singularity is reflected in the singular behavior of the perturbation modes $\varphi_{(n)}$ near the south pole of the HM instanton $\bar\eta = \pi/H_n$. Even though the unbounded growth of the perturbation modes signals the breakup of perturbation theory, the behavior of the lowest order singular mode is likely to determine the singular behavior of the full solution. In the case of $n = 1$ solutions, the third mode $\varphi_{(3)}$ is the lowest order singular mode [36]:

$$\begin{aligned} \varphi_{(3)} &\overset{\eta\to\bar\eta}{\propto} -\frac{32 + \nu^2 + 18\lambda}{(\bar\eta - \eta)^2}\,, && (51)\\ \nu &\equiv \frac{2V^{(3)}_{top}}{\kappa^{1/2}\mu^2}\,, && (52)\\ \lambda &\equiv \frac{2V^{(4)}_{top}}{3\kappa\mu^2}\,. && (53)\end{aligned}$$

The transition between the overshooting ($n = 1$) and undershooting ($n = 2$) behaviors corresponds to change in the sign of the divergence of $\varphi_{(3)}$:

$$8\kappa\,\mu^4_{c,1} + 3V^{(4)}_{top}\,\mu^2_{c,1} + (V^{(3)}_{top})^2 = 0\,. \tag{54}$$

In our case $\kappa = 1$, $V^{(4)}_{top} = -6$ and $V^{(3)} = 0$:

$$\mu^2_{c,1} = \frac{9}{4}\,. \tag{55}$$

This result can be stated differently, saying that when the fourth derivative of the potential φ_{top} is more negative than the critical value:

$$V^{(4)}_c = -\frac{8\kappa\mu^2_{c,1}}{3} - \frac{(V^{(3)}_{top})^2}{3\mu^2_{c,1}}\,, \tag{56}$$

new $n = 1$ instanton solutions appear in a class of theories with $n_{top} \lesssim 1$. The critical value (54) can be derived in a more rigorous way by studying the properties of the action functional in the vicinity of the critical HM solution [37]. Using similar techniques, one can prove analytically that $n = 1$ istantons appearing at small $(\varphi_0 - \varphi_{top})$ when $\mu^2 \lesssim \mu^2_{c,1}$ always have greater euclidean action than the corresponding HM solutions [38], which we numerically verified (see Figure 6, center panel).

In conclusion, when the curvature μ^2 of the potential at its top is nonzero, the small–$(\varphi_0 - \varphi_{top})$ solutions can be studied as small perturbations of the critical HM solution. However, focusing on the $n = 1$ solutions, when $\mu^2 \ll \mu_{c,1}$,

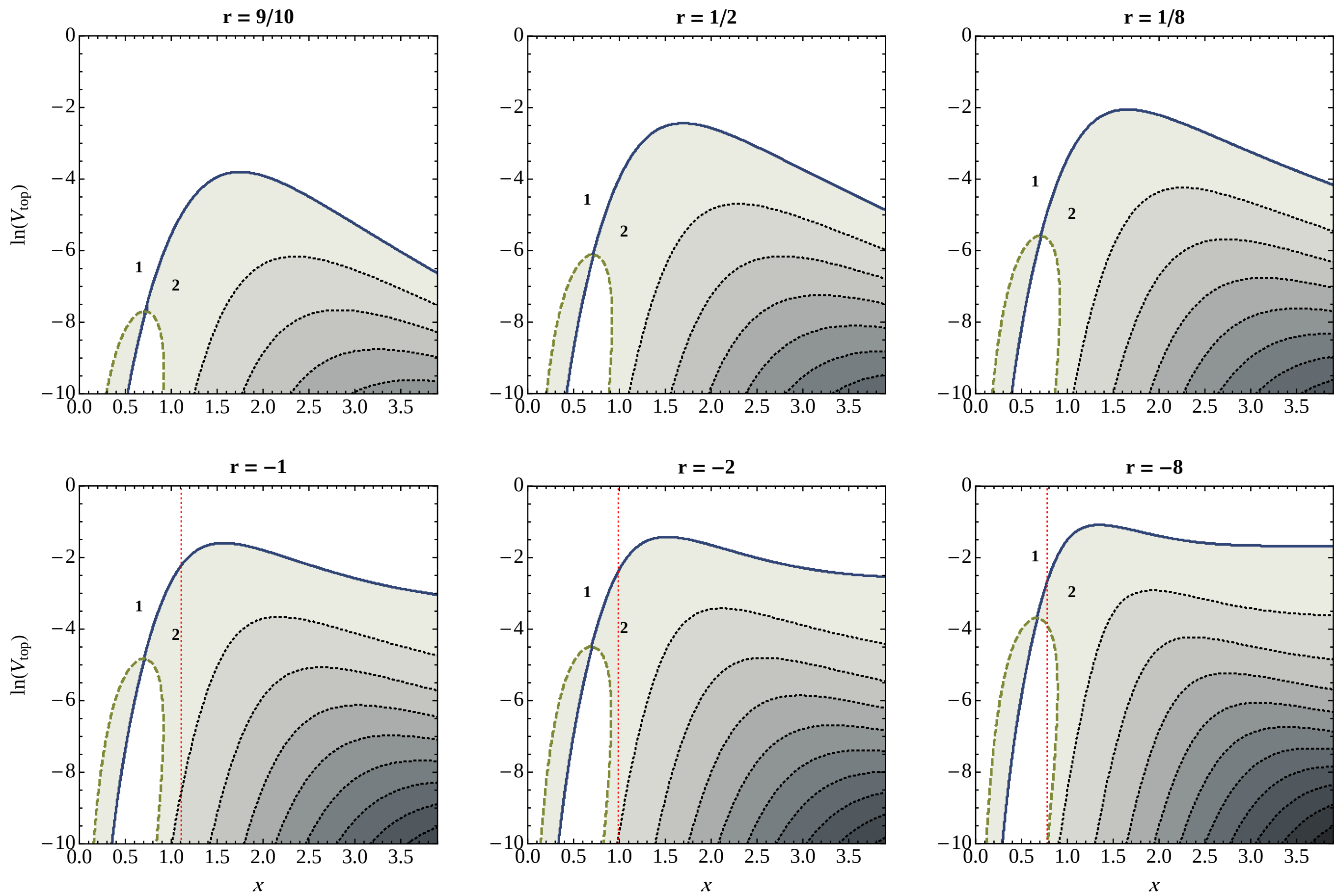

Figure 7: Instanton diagrams for the potential (57) and different values of the ratio (58). The red, dotted lines represent $V(\varphi_0) = 0$.

the position of the critical point A_1 remains approximately fixed (see Figure 5) and, over a wide range of values for V_{top}, non–standard $n = 1$ solutions are found which cannot be described as perturbations of HM. The existence of the ring–like structure and the non–symmetric branch therein are a striking manifestation of this fact. This suggests, in agreement with the expectation expressed in [7], that the existence of these non–standard branches cannot be directly related to the shape of the potential at $\varphi = \varphi_{top}$, but is rather determined by the full structure of the potential.

VI. MORE REALISTIC FLAT POTENTIALS

A. Positive potentials

In the previous two sections, we studied the existence of instanton solutions connecting vacua separated by flat and nearly flat potential barriers. However, as illustrated in Figures 3 and 5, most of these solutions extend to ranges of field space in which $V < 0$. In order to clarify the role of these negative values of V in the existence of non–standard $n_{top} < 1$ solutions, we considered a regularized version of the scalar potential (30):

$$V = V_{top} - \frac{\lambda}{4}\varphi^4 + \frac{t}{6}\varphi^6 \,. \tag{57}$$

Via the rescalings (33) we set again $\lambda = \kappa = 1$. In order to consider a class of theories with $V > 0$ and let V_{top} vary, we parametrically fix t so as to keep the ratio between the vacuum energy densities at the degenerate vacua $\varphi_\pm$ and at φ_{top} constant:

$$r = V_\pm / V_{top} \,. \tag{58}$$

When $r < 0$, one has $V_\pm < 0$ and non–compact solutions could exist for which the scalar field approaches φ_+ or φ_- asymptotically. However, for such a non–compact solution the quantity $\frac{1}{2}\varphi'^2 - V$ is decreasing, and its asymptotic

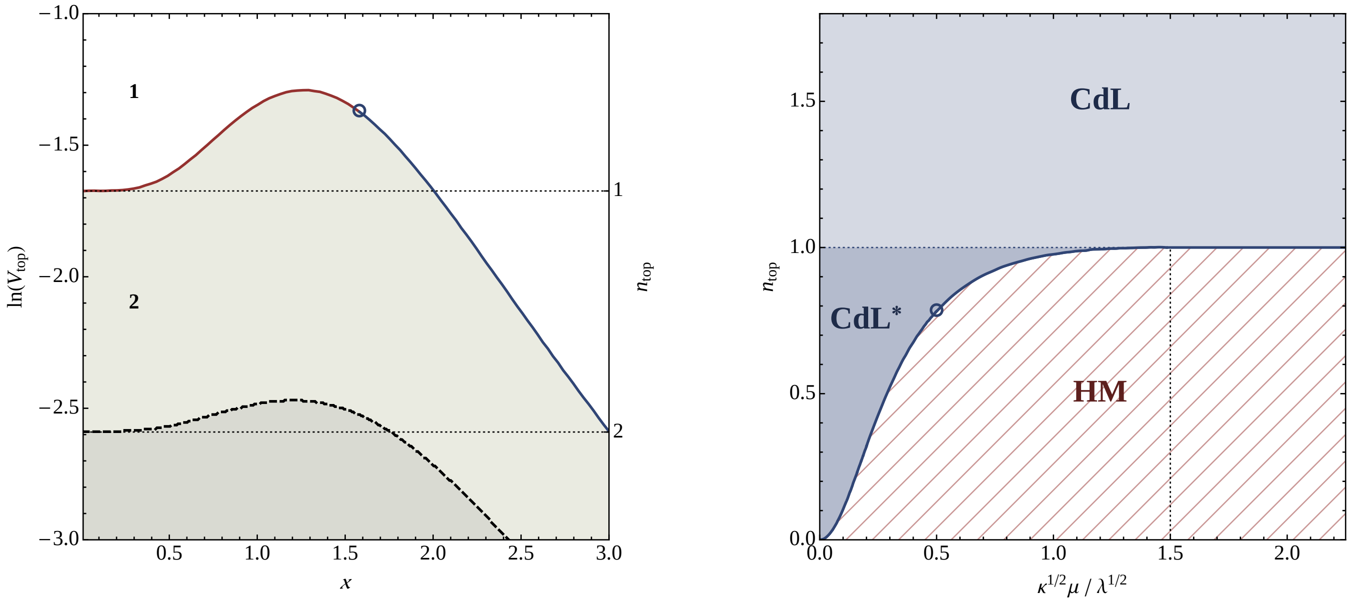

Figure 8: Left panel: instanton diagram for the theory (60) with $r = 1/4$, $\mu = 0.5$ and the choice of units $\lambda = \kappa = 1$. The blue curve on the right of the highlighted point represents $n = 1$ solutions with more negative euclidean action than the HM solution at equal V_{top}. Right panel: phase diagram for the dominant tunneling channel for the potential (60) with $r = 1/4$. For $\mu < \mu_{c,1} = 3/2$ (55), $n = 1$ instantons with $n_{top} < 1$ persist which dominate the decay rate. The highlighted point corresponds to the solution depicted on the left panel.

value $V_+ = V_-$ is necessarily smaller than its initial value V_0. In the case of our potential $V \geq V_\pm$ and the only non–compact solutions are the euclidean–AdS $\varphi(\eta) = \varphi_\pm$ solutions.

In Figure 7 we present instanton diagrams for several values of r. The reduced field variable x already introduced in Section III is used in order to visualize solutions which have φ_0 very close to the true vacuum value φ_+:

$$\varphi_0 \equiv \varphi_+ \left(1 - e^{-x^2}\right) . \tag{59}$$

The left part of the diagrams show a clear resemblance with the one describing the $V = V_{top} - \varphi^4/4$ case. In particular, the bifurcation along the $n = 1$ branch remains visible. We also checked that, by adding a small mass term, the ring structure described in the previous section appear at least along the $n = 1$ branch. This suggests that the features of the non–standard branches are not related to negative values of the potential. Indeed, the appearance of a bifurcation point had first been noticed in the case of a positive potential [7]. At the same time, as expected from the overshooting argument, when $r > 0$ all the instanton curves bend down as x increases, in such a way that $n(\varphi_+ - \epsilon, V_{top}) = 1$ for any value of V_{top}. In this respect, the large x part of these instanton diagrams is analogous to the one for the standard CdL case (see Figure 2). On the other hand, when $r < 0$ the curves appear again to approach constant values of V_{top} as in Figure 3, which described the $r = -\infty$ case.

Focusing on the $r > 0$ case, we stress again that in the presence of a flat potential barrier, for sufficiently small V_{top} non–standard solutions coexist with standard CdL–type solutions with φ_0 very close to φ_+. The existence of both types of solutions in spite of the flatness of the potential barrier ($n_{top} = 0$ in the present case) can be related to the presence of the critical solution sitting at the top of each instanton curve. The euclidean action and the number of negative modes of these solutions follow the behaviors already described in Section IV. In particular, as already noticed in [38] for a potential with $n_{top} \lesssim 1$, "standard" $n = 1$ solutions located sufficiently at the right of the critical points have more negative euclidean action than the corresponding HM solutions. Possessing a single negative mode, these solutions are the dominant tunneling channel for this class of theories.

As expected from the results of the previous section, this qualitative picture remains valid even if the potential is not exactly flat at $\varphi = \varphi_{top}$, e.g.:

$$V = V_{top} - \frac{\mu^2}{2} - \frac{\lambda}{4}\varphi^4 + \frac{t}{6}\varphi^6 . \tag{60}$$

Once again, t can be parametrically fixed in terms of μ and λ so as to keep the ratio $r = V_+/V_{top}$ constant. For $\mu < \mu_{c,1}$ (54), standard $n = 1$ instantons still exist when $n_{top} < 1$. Moreover, sufficiently far from the critical point these solutions start having more negative euclidean action than HM (see Figure 8, left panel) and give the dominant contribution to the tunneling rate. The phase diagram on the right panel of Figure 8 describes the dominant decay

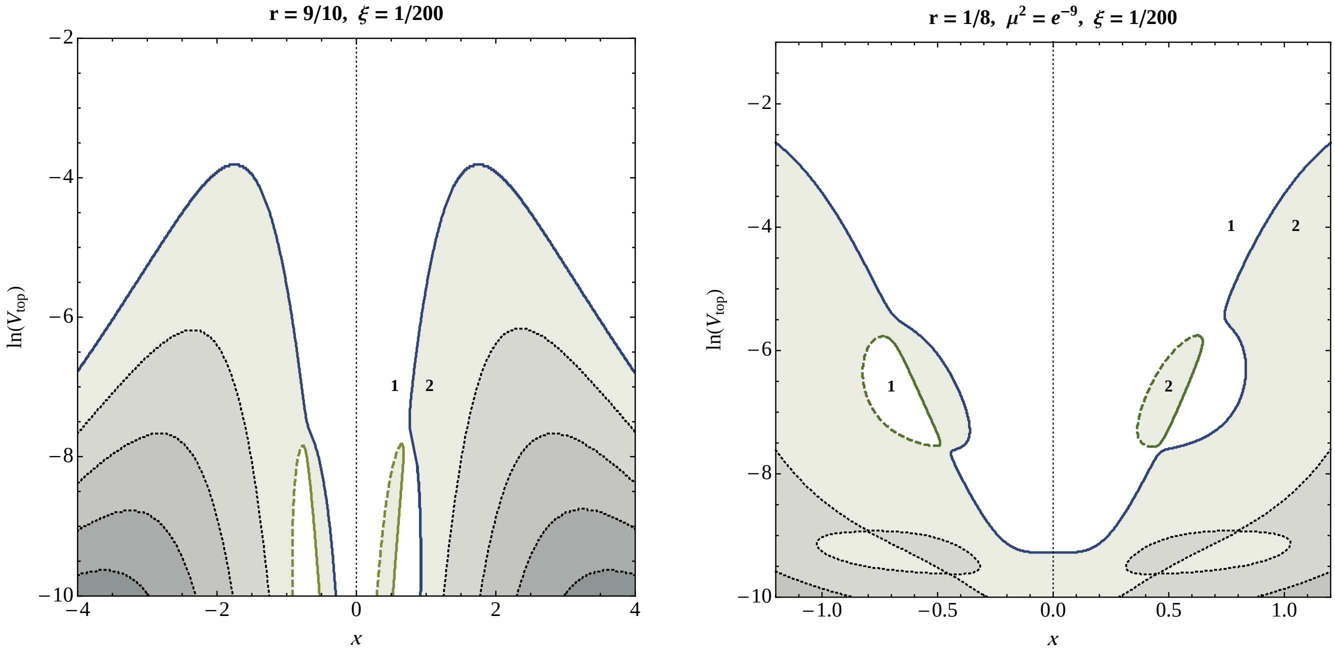

Figure 9: Left panel: instanton diagram for the potential (61), with $r = 9/10$, $\mu^2 = 0$ and $\xi = 1/200$. For the $n = 1$ solutions, the scalar field varies between the values at $x > 0$ and the corresponding values at $x < 0$: different colors and dashing represent the correspondence between the various branches. Right panel: detail of the instanton diagram for $r = 1/8$, $\mu^2 = e^{-9}$ and $\xi = 1/200$. The second bifurcation point also becomes a simple critical point and an "island" forms in the (x, V_{top}) plane.

channel for the class of theories (60). CdL instantons exist and dominate the decay rate not only when $n_{top} > 1$, but also for flatter barriers provided the fourth derivative of the potential at φ_{top} is sufficiently negative to allow the presence of a new critical instanton. As we will show in Section VII, such critical solutions are present also for flatter potentials for which $V^{(4)}(\varphi_{top}) = 0$: therefore, the persistence and dominance of CdL solutions below $n_{top} = 1$ illustrated in Figure 8 should not be regarded as a consequence of the large, negative values of $V^{(4)}(\varphi_{top})$.

B. Asymmetric potentials

The flat or approximately flat potentials considered so far were taken to be symmetric under $\varphi \to \varphi_{top} - \varphi$. In this section we briefly highlight the changes to the previous pictures when a small asymmetry is added. We consider the potential:

$$V = V_{top} - \frac{\mu^2}{2}\varphi^2 - \frac{\lambda}{4}\varphi^4 - \frac{\xi\, t^{1/2}}{5}\varphi^5 + \frac{t}{6}\varphi^6 \,, \tag{61}$$

and once again fix t parametrically so as to keep the ratio $r = V_+/V_{top}$ fixed. The left panel of Figure 9 represents the instanton diagram for the class of theories with $\xi = 1/200$ and $r = 9/10$. The reduced variable x was defined in Eq. (21) in Section III. Interestingly, the addition of a small asymmetry causes the disappearance of the bifurcation point, which transforms into a simple critical point. Because of the asymmetry, none of the instanton profiles is exactly symmetric under $\eta \to \bar{\eta} - \eta$. This explains how the previously symmetric branch lying above the bifurcation point now extends smoothly into the previously asymmetric branch. As the asymmetry is increased, the critical point moves further away from the $n = 1$ branch connected to the CdL–type solutions. The number of negative modes along each of the branches is the same as in the $\xi = 0$ case.

When a small mass term is added the second bifurcation point presented in Figure 6 also appears as a simple critical point, and an "island" replaces the ring–like structure observed in the symmetric case (compare the right panel of Figure 9 with the left panel of Figure 6). As the coefficient of the mass term is increased, the size of these islands shrinks progressively until their complete disappearance.

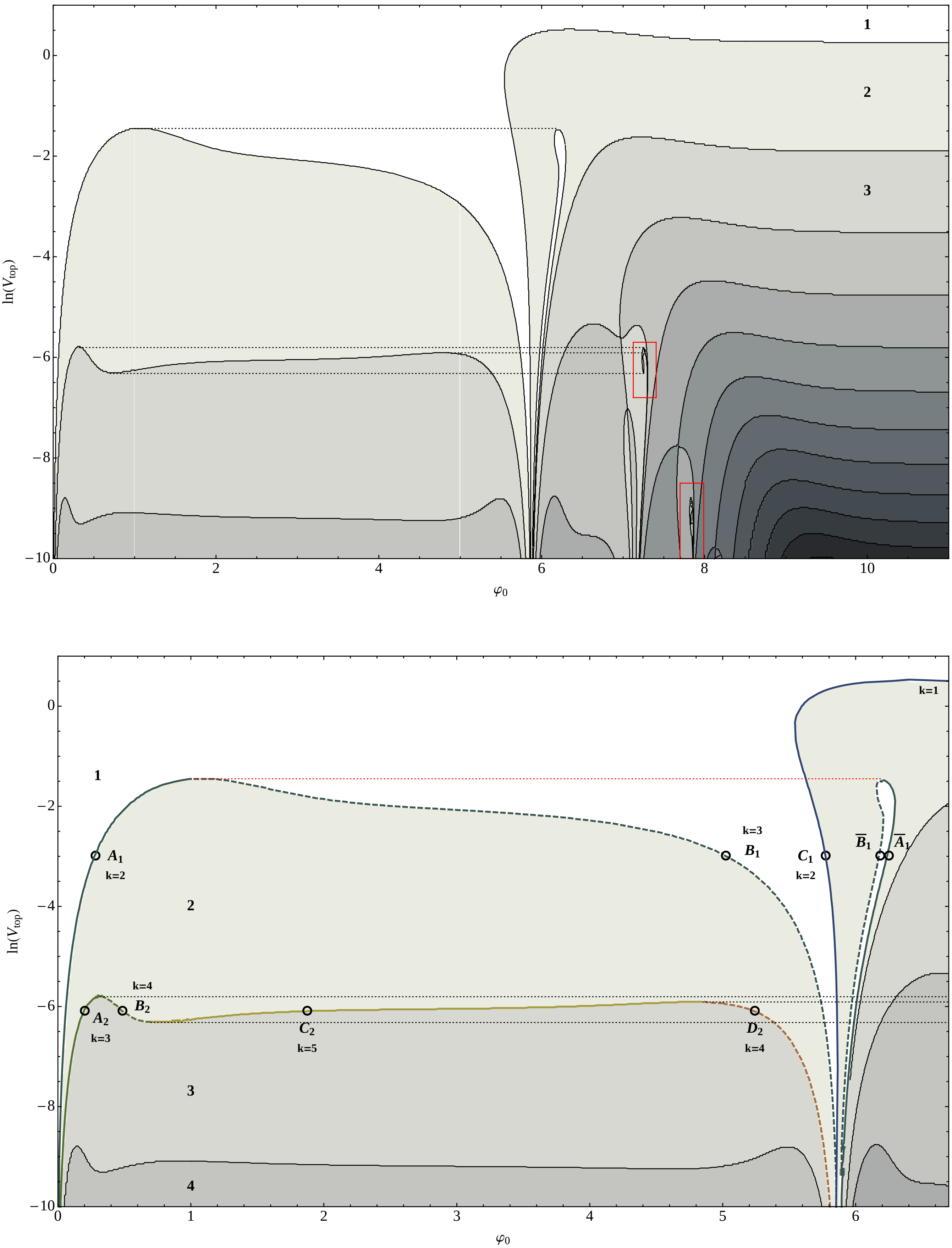

Figure 10: Two views of the instanton diagram for the potential (62), $\kappa = \lambda = 1$. The two regions higlighted in the top panel correspond to the diagrams in Figure 11. The highlighted points, the colors and the dashing in the bottom panel correspond to the same elements in the left panel of Figure 11. The number of negative modes for some branches is also indicated.

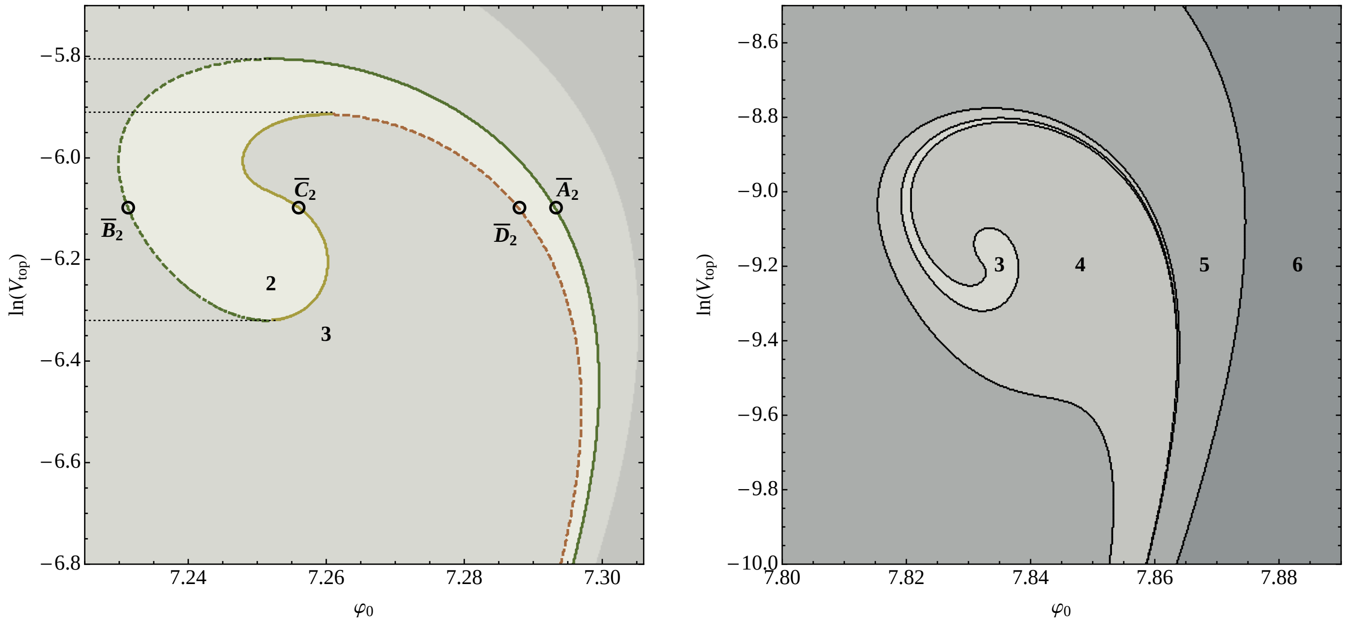

Figure 11: Two details of the instanton diagrams in Figure 10. The highlighted points correspond to those in the bottom panel of Figure 10 under the transformation $\varphi(\eta) \to -\varphi(\bar{\eta} - \eta)$.

VII. HIGHER ORDER FLATNESS: $V = V_{top} - \frac{1}{6}\varphi^6$

As we have seen, the existence of instantons for potentials with $n_{top} < 1$ can be related, in the vicinity of the critical HM solutions, to the presence of a large and negative fourth derivative term in the expansion of the potential near φ_{top}. To complete our overview of instanton solutions in the presence of flat potential barriers, we studied a class of potentials for which $V^{(4)}_{top}$ vanishes, and the potential barrier is even flatter:

$$V = V_{top} - \frac{\lambda}{6}\varphi^6 \,. \tag{62}$$

By an appropriate choice of units one may again set $\lambda = \kappa = 1$. Figures 10 and 11 present different regions of the instanton diagram corresponding to the family of theories (62).

From the very rich structure of the diagram we can extract the following observations:

- at large φ_0, the approximately shift-symmetric pseudo–inflationary solutions in the euclidean potential $-V$ are again present. These solutions are exactly symmetric across $\varphi = 0$, and have as many negative modes as oscillations ($k = n$).
- many additional critical instantons appear. Correspondingly, new branches at smaller φ_0 are present for every visible value of n. Most of these branches, just as in the case of a $-\varphi^4$ potential, correspond to asymmetric solutions. For example, the $n = 1$ solutions A_1 and B_1 correspond to $\bar{A}_1$ and $\bar{B}_1$ under the transformation $\varphi(\eta) \to -\varphi(\bar{\eta} - \eta)$.
- several bifurcation points are visible on the $n = 3$ and $n = 5$ curves in the top panel of Figure 10.

The most surprising feature emerging from the instanton diagrams is the chaotic character of the landscape of solutions: for example, the solutions corresponding to the rather separated points A_1 and B_1 end on the field values corresponding to $\bar{A}_1$ and $\bar{B}_1$. Furthermore, as V_{top} decreases the distance in field space between A_1 and B_1 remains approximately constant, while $\bar{A}_1$ and $\bar{B}_1$ approach each other. The chaotic behavior is displayed even more clearly by the $n = 2$ solutions A_2, B_2, C_2 and D_2. These represent further asymmetric solutions, and their conjugated points lie on the very small structure depicted in the left panel of Figure 11. A similar structure appears for the $n = 3$ solutions (Figure 11, right panel).

These result indicate that a rich structure of instanton solutions in theories with $n_{top} < 1$ can be found without the presence of a large fourth derivative term at $\varphi = \varphi_{top}$. Moreover, when the potential is dominated by a $-\varphi^6$ term around the top of the barrier, the non–linearity of the field equations allows a very complicated landscape of solutions which, however, are not directly relevant for vacuum decay, having more than one negative mode and larger euclidean action than HM. As a final application and in the same spirit as in Section VI, we checked that if a regularization is added so as to make the potential positive definite,

$$V = V_{top} - \frac{\lambda}{6}\varphi^6 + \frac{t}{8}\varphi^8 \ , \tag{63}$$

the complex structure of the instanton diagram in Figure 10 does not disappear.

VIII. CONCLUDING REMARKS

Our systematic investigation of instantons in Einstein gravity coupled to a single self-interacting scalar field theory with relatively flat potentials shows the existence of a very complex landscape of solutions. We studied in detail the solutions appearing with quartic and higher order potentials, with and without mass term, and investigated the influence of potential regularizations and asymmetries on the instantons properties.

Our study highlights the role of critical instantons as keystones for the existence of non–standard branches of solutions. The existence of one or more critical instantons appears as a general feature of flat or almost flat potentials and, as our results for the sextic potential illustrate, does not depend on a large negative value of the fourth derivative of the potential at the top. The new branches that emanate from these critical points typically contain more than one negative mode in their spectrum of fluctuations, indicating that one may expect solutions with fewer negative modes and lower action nearby. We have found that, in the case that the potential is regularized so as to contain a minimum at positive values of the potential, ordinary CdL instantons always persist near these minima, and they typically provide the dominant contribution to the decay rate out of these vacua.

Close to the top of the potential barrier, critical instantons are also associated to new instanton branches with a small field excursion and additional negative modes, which connect to the critical HM solution when a small curvature term is added to the potential. The non–linear character of these new branches is indicated by the presence of bifurcation points, which we showed to be related to the exact symmetry of the potential, and of a very complex space of solutions in the $V = V_{top} - \frac{1}{6}\varphi^6$ case. We showed that these features appear regardless of the positive definiteness of the scalar potential.

There are several open questions related to our research. An obvious one is to ask whether or not the complexity remains for potentials with an even higher degree of flatness – we strongly suspect that it does. Furthermore, given that our investigation was mainly numerical, it would be interesting to see if one could obtain some of these instanton solutions analytically. For instance, it may perhaps be possible to determine the critical instantons analytically as fixed points of a corresponding dynamical system.

The most important question is probably the issue of what the correct interpretation and physical relevance of these new branches of solutions are. In particular, it would be interesting to know whether the new branches contribute to metastable vacuum decay. There are two extreme viewpoints on this subject. According to the "orthodox" view [39], euclidean solutions with more than one negative mode have nothing to do with tunneling. However, one should bear in mind that this statement was only proven in the absence of gravity, which leaves some room for speculation. Recently in the context of oscillating instantons a more "heretic" viewpoint was discussed in [40], where it was conjectured that the existence of numerous solutions with various numbers of negative modes might sum up in the functional integral and give a contribution to decay rates. An interesting challenge for future investigations will be to clarify these issues, and to determine the physical role of these intricate solutions.

Acknowledgements

G.L. is thankful to the Quantum Gravity group of the Albert-Einstein-Institute and especially Hermann Nicolai for kind hospitality during his visit to Potsdam. L.B. and J.L.L. gratefully acknowledge the support of the European Research Council via the Starting Grant numbered 256994.

Appendix A: Singularities in instanton solutions

1. No singularities at finite ρ

First, we prove that, if the potential V is regular everywhere, solutions of (7, 8) cannot become singular at a finite value of ρ. This is a slight generalization of the proof presented in [17], where the potential was taken to be bounded. Let $n(\eta) \equiv \log \rho(\eta)$ be well–defined for $\eta < 0$ so that $\eta = 0$ is the candidate singular point. To facilitate reading we reproduce the field equations in both their forms:

$$\varphi'' = -3\frac{\rho'}{\rho}\varphi' + V_{,\varphi} = -3N'\varphi' + V_{,\varphi} \,, \tag{A1}$$

$$\frac{\rho'^2}{\rho^2} = \frac{1}{\rho^2} + \frac{\kappa}{3}\left(\frac{1}{2}\varphi'^2 - V\right) , \tag{A2}$$

$$N'^2 = e^{-2N} + \frac{\kappa}{3}\left(\frac{1}{2}\varphi'^2 - V\right) , \tag{A3}$$

$$N'' = -e^{-2N} - \frac{\kappa\varphi'^2}{2} \,. \tag{A4}$$

From (A4) we know that $N(\eta)$ is a concave function. Therefore, only two cases are possible:

1. N' approaches a finite constant as $\eta \to 0^-$,
2. $N' \to -\infty$ as $\eta \to 0^-$.

In the first case, the singularity must show up in the behavior of the scalar field φ. However, possible divergences in V and φ' are then related by (A3):

$$\lim_{\eta\to 0^-}\left(\frac{1}{2}\varphi'^2 - V\right) = N_0'^2 - e^{-2N_0} \,, \tag{A5}$$

where zero indices denote quantities evaluated at $\eta = 0$. In the vicinity of $\eta = 0$, the equation for the scalar field is that of a particle in a potential $-V$ with a friction force proportional to its speed, and constant coefficient $3N_0'$. Therefore, a singularity in the scalar field can only be driven by the potential diverging as $\varphi \to \pm\infty$. However, the divergence of φ requires φ' to diverge at least as η^{-1}. Equation (A4) then implies that N' is also divergent near $\eta = 0$,

$$N'' \leq -\frac{\kappa\varphi'^2}{2} \propto -\frac{1}{\eta^2} \,, \tag{A6}$$

which contradicts our initial hypothesis. In other words, if the scalar field diverges due to an instability of the euclidean potential $-V$, ρ'/ρ also diverges near the singular point. Now, we want to exclude the possibility that this divergence could take place at finite ρ.

Let's suppose now that $N \to N_0 > 0$ while $N' \to -\infty$. Because n is a convex function, we can assume the asymptotic behavior

$$N \simeq N_0 + \alpha\,(-\eta)^p, \quad 0 < p < 1 \,. \tag{A7}$$

Inserting this behavior in (A4), we find

$$|\varphi'| \sim (-\eta)^{-1+p/2} \,. \tag{A8}$$

This can be plugged back into (A1), resulting in

$$|V_{,\varphi}| \sim (-\eta)^{-2+p/2} \,. \tag{A9}$$

For a regular potential this kind of divergence is only possible as $\varphi \to \pm\infty$, which is however not attainable when $\eta \to 0^-$ because (A8) implies that the scalar field "speed" φ' does not diverge fast enough.

2. Singular instantons and runaway of the scalar field

Following the results of Appendix A 1, only compact solutions of the equations for $O(4)$–invariant instantons can be singular. Moreover, the singularities are all characterized by

$$\rho \overset{\eta\to 0^-}{\longrightarrow} 0 \,, \tag{A10}$$

taking ρ to be regular for $\eta < 0$. We now show the relation between the behavior of the scalar field and of the metric function ρ near the point $\rho = 0$, both in the singular and non–singular case.

Suppose first that $\varphi \to \varphi_0$ as $\eta \to 0^-$, where φ_0 is some finite value. In this case, the derivative combination $\frac{\rho'}{\rho}\varphi'$ must remain finite, otherwise the asymptotic scalar field equation (A1) would read

$$\varphi'' \simeq -3\frac{\rho'}{\rho}\varphi' \quad \Rightarrow \quad \varphi' \propto \rho^{-3} , \tag{A11}$$

In this case, the asymptotic form of (A2) reads

$$\rho'^2 \propto \rho^{-4} \quad \Rightarrow \quad \rho \propto (-\eta)^{1/3} . \tag{A12}$$

In this case, however, $\varphi' \propto (-\eta)^{-1}$ and φ diverges logarithmically, which contradicts our initial hypothesis. Therefore, if the solution is such that φ approaches a finite value, the combination $\frac{\rho'}{\rho}\varphi'$ must approach a finite value. As ρ'/ρ is diverging monotonically, this requires φ' to approach zero, in which case one also finds from (A2)

$$\rho' \overset{\eta\to 0^-}{\longrightarrow} 1 . \tag{A13}$$

This means that whenever φ approaches a finite constant the solution is actually fully non–singular.

The nature of the singularity appearing in compact solutions with φ diverging as $\rho \to 0$ might depend on the asymptotics of the scalar field potential. However, for potentials which are bounded or which diverge (positive or negative) with a power law, one can easily check that

$$\rho \;\propto\; (\bar\eta - \eta)^{1/3} , \tag{A14}$$
$$\varphi \;\propto\; \log(\bar\eta - \eta) , \tag{A15}$$

is a an asymptotic solution of the field equations. From the point of view of the scalar field equation (A1), this means that provided the potential is not too steep the divergence of φ is always asymptotically driven by the anti–friction term $-3\frac{\rho'}{\rho}\varphi'$.

Appendix B: Continuous families of solutions and perturbation modes

In Section III B we stated that when the instanton curve $V_{top}(\varphi_0)$ has a stationary point at φ_0^*, the solution corresponding to this value of φ_0 possesses a regular perturbation mode. In this section we prove this statement in the simplified context of a theory with no reparametrization invariance.

Let $S[\varphi(x), p]$ be an action which depends *explicitly* on some real parameter p. Let now $\varphi_\lambda(x)$ be a family of solutions for the family of theories specified by $S[\varphi, p(\lambda)]$. Finally, let's assume $\varphi_\lambda(x)$ to be a regular function of λ. We prove that, if $p'(\lambda^*) = 0$, then

$$\partial_\lambda \varphi(x)\Big|_{\lambda=\lambda^*}$$

is a regular perturbation mode of φ_{λ^*}. Let $\delta\varphi$ be a generic field variation. We now assume t to be infinitesimal and consider the quantity

$$\begin{aligned} S\Big[\varphi_{\lambda^*+\delta\lambda} + t\,\delta\varphi, p(\lambda^*+\delta\lambda)\Big] &= S\Big[\varphi_{\lambda^*} + t\,\delta\varphi + \delta\lambda(\partial_\lambda\varphi_\lambda)|_{\lambda=\lambda^*}, p(\lambda^*)\Big] + \mathcal{O}(\delta\lambda^2) \\ &= S[\varphi_{\bar\lambda}, p(\lambda^*)] + \mathcal{O}(t^2, \delta\lambda^2) \\ &\quad + t\,\delta\lambda \int d^4x\, d^4y\, \delta\varphi(x) \frac{\delta^2 S[\varphi_{\lambda^*}, p(\lambda^*)]}{\delta\varphi(x)\delta\varphi(y)} (\partial_\lambda\varphi_\lambda)|_{\lambda=\lambda^*}(y) . \end{aligned}$$

Of course, no terms in t and $\delta\lambda$ are present because of the field equations for φ_{λ^*}. On the other hand, the field equation for $\varphi_{\bar\lambda+\delta\lambda}$ implies

$$\frac{dS[\varphi_{\lambda^*+\delta\lambda} + t\,\delta\varphi, p(\bar\lambda+\delta\lambda)\Big]}{dt}\Big|_{t=0} = 0 . \tag{B1}$$

At order $\delta\lambda$, this implies

$$\int d^4x\, d^4y\, \delta\varphi(x) \frac{\delta^2 S[\varphi_{\lambda^*}, p(\lambda^*)]}{\delta\varphi(x)\delta\varphi(y)} (\partial_\lambda\varphi_\lambda)|_{\lambda=\lambda^*}(y) = 0 . \tag{B2}$$

As $\delta\varphi(x)$ is a generic field variation, this implies that $(\partial_\lambda\varphi_\lambda)|_{\lambda=\lambda^*}$ is a regular perturbation of φ_{λ^*}

$$\int d^4y \frac{\delta^2 S[\varphi_{\lambda^*}, p(\lambda^*)]}{\delta\varphi(x)\delta\varphi(y)}(\partial_\lambda\varphi_\lambda)|_{\lambda=\lambda^*}(y) = 0\ . \tag{B3}$$

---

[1] S. R. Coleman and F. De Luccia, "Gravitational Effects on and of Vacuum Decay," *Phys. Rev.* **D21** (1980) 3305.
[2] S. R. Coleman, "The fate of the false vacuum. 1. semiclassical theory," *Phys.Rev.* **D15** (1977) 2929–2936.
[3] S. Hawking and I. Moss, "Supercooled Phase Transitions in the Very Early Universe," *Phys.Lett.* **B110** (1982) 35.
[4] E. J. Weinberg, "Hawking-Moss bounces and vacuum decay rates," *Phys.Rev.Lett.* **98** (2007) 251303, arXiv:hep-th/0612146 [hep-th].
[5] R. Bousso and J. Polchinski, "Quantization of four form fluxes and dynamical neutralization of the cosmological constant," *JHEP* **0006** (2000) 006, arXiv:hep-th/0004134 [hep-th].
[6] M. R. Douglas, "The Statistics of string / M theory vacua," *JHEP* **0305** (2003) 046, arXiv:hep-th/0303194 [hep-th].
[7] J. C. Hackworth and E. J. Weinberg, "Oscillating bounce solutions and vacuum tunneling in de Sitter spacetime," *Phys.Rev.* **D71** (2005) 044014, arXiv:hep-th/0410142 [hep-th].
[8] A. R. Brown and E. J. Weinberg, "Thermal derivation of the Coleman-De Luccia tunneling prescription," *Phys.Rev.* **D76** (2007) 064003, arXiv:0706.1573 [hep-th].
[9] A. R. Brown and A. Dahlen, "The case of the disappearing instanton," *Phys.Rev.* **D84** (2011) 105004, arXiv:1106.0527 [hep-th].
[10] J. Garriga and A. Vilenkin, "Recycling universe," *Phys.Rev.* **D57** (1998) 2230–2244, arXiv:astro-ph/9707292 [astro-ph].
[11] J. Garriga, D. Schwartz-Perlov, A. Vilenkin, and S. Winitzki, "Probabilities in the inflationary multiverse," *JCAP* **0601** (2006) 017, arXiv:hep-th/0509184 [hep-th].
[12] B. Freivogel, M. Kleban, M. Rodriguez Martinez, and L. Susskind, "Observational consequences of a landscape," *JHEP* **0603** (2006) 039, arXiv:hep-th/0505232 [hep-th].
[13] M. C. Johnson and J.-L. Lehners, "Cycles in the Multiverse," *Phys.Rev.* **D85** (2012) 103509, arXiv:1112.3360 [hep-th].
[14] J.-L. Lehners, "Eternal Inflation With Non-Inflationary Pocket Universes," *Phys.Rev.* **D86** (2012) 043518, arXiv:1206.1081 [hep-th].
[15] L. G. Jensen and P. J. Steinhardt, "Bubble nucleation for flat potential barriers," *Nucl.Phys.* **B317** (1989) 693–705.
[16] L. Battarra, G. Lavrelashvili, and J.-L. Lehners, "Negative modes of oscillating instantons," *Phys.Rev.* **D86** (2012) 124001, arXiv:1208.2182 [hep-th].
[17] R. Bousso, B. Freivogel, and M. Lippert, "Probabilities in the landscape: The decay of nearly flat space," *Phys.Rev.* **D74** (2006) 046008, arXiv:hep-th/0603105 [hep-th].
[18] A. Khvedelidze, G. V. Lavrelashvili, and T. Tanaka, "On cosmological perturbations in closed frw model with scalar field and false vacuum decay," *Phys.Rev.* **D62** (2000) 083501, arXiv:gr-qc/0001041 [gr-qc].
[19] G. V. Lavrelashvili, "Negative mode problem in false vacuum decay with gravity," *Nucl.Phys.Proc.Suppl.* **88** (2000) 75–82, arXiv:gr-qc/0004025 [gr-qc].
[20] S. Gratton and N. Turok, "Homogeneous modes of cosmological instantons," *Phys.Rev.* **D63** (2001) 123514, arXiv:hep-th/0008235 [hep-th].
[21] G. Lavrelashvili, "The Number of negative modes of the oscillating bounces," *Phys.Rev.* **D73** (2006) 083513, arXiv:gr-qc/0602039 [gr-qc].
[22] G. V. Dunne and Q.-h. Wang, "Fluctuations about Cosmological Instantons," *Phys.Rev.* **D74** (2006) 024018, arXiv:hep-th/0605176 [hep-th].
[23] V. Balek and M. Demetrian, "A criterion for bubble formation in de sitter universe," *Phys.Rev.* **D69** (2004) 063518, arXiv:gr-qc/0311040 [gr-qc].
[24] S. Fubini, "A New Approach to Conformal Invariant Field Theories," *Nuovo Cim.* **A34** (1976) 521.
[25] A. Belavin, A. M. Polyakov, A. Schwartz, and Y. Tyupkin, "Pseudoparticle Solutions of the Yang-Mills Equations," *Phys.Lett.* **B59** (1975) 85–87.
[26] I. Affleck, "On Constrained Instantons," *Nucl.Phys.* **B191** (1981) 429.
[27] K.-M. Lee and E. J. Weinberg, "Tunneling without barriers," *Nucl.Phys.* **B267** (1986) 181.
[28] K.-M. Lee, "Tunneling without barriers in curved space-time," *Nucl.Phys.* **B282** (1987) 509.
[29] A. D. Linde, "Particle physics and inflationary cosmology," *Contemp.Concepts Phys.* **5** (1990) 1–362, arXiv:hep-th/0503203 [hep-th].
[30] J. L. Barbon and E. Rabinovici, "Holography of AdS vacuum bubbles," *JHEP* **1004** (2010) 123, arXiv:1003.4966 [hep-th].
[31] J. Barbon and E. Rabinovici, "AdS Crunches, CFT Falls And Cosmological Complementarity," *JHEP* **1104** (2011) 044, arXiv:1102.3015 [hep-th].
[32] S. de Haro, I. Papadimitriou, and A. C. Petkou, "Conformally Coupled Scalars, Instantons and Vacuum Instability in AdS(4)," *Phys.Rev.Lett.* **98** (2007) 231601, arXiv:hep-th/0611315 [hep-th].
[33] S. de Haro and A. C. Petkou, "Instantons and Conformal Holography," *JHEP* **0612** (2006) 076, arXiv:hep-th/0606276 [hep-th].
[34] F. Loran, "Fubini vacua as a classical de Sitter vacua," *Mod.Phys.Lett.* **A22** (2007) 2217–2235, arXiv:hep-th/0612089

[hep-th].
[35] B.-H. Lee, W. Lee, C. Oh, D. Ro, and D.-h. Yeom, "Fubini instantons in curved space," *JHEP* **1306** (2013) 003, arXiv:1204.1521 [hep-th].
[36] T. Tanaka and M. Sasaki, "False vacuum decay with gravity: Negative mode problem," *Prog.Theor.Phys.* **88** (1992) 503–528.
[37] V. Balek and M. Demetrian, "Euclidean action for vacuum decay in a de sitter universe," *Phys.Rev.* **D71** (2005) 023512, arXiv:gr-qc/0409001 [gr-qc].
[38] M. Demetrian, "False vacuum decay with gravity in a critical case," *Int.J.Theor.Phys.* **46** (2007) 652–663, arXiv:gr-qc/0504133 [gr-qc].
[39] S. R. Coleman, "Quantum tunneling and negative eigenvalues," *Nucl.Phys.* **B298** (1988) 178.
[40] B.-H. Lee, W. Lee, and D.-h. Yeom, "Oscillating instantons as homogeneous tunneling channels," *Int. J. Mod. Phys.* **A28** (2013) 1350082, arXiv:1206.7040 [hep-th].